67th International Astronautical Congress (IAC), Guadalajara, Mexico, 26-30 September 2016.

IAC-16,A7,2,2,x32004
A Novel Orbiter Mission Concept for Venus with the EnVision Proposal

Marta R. R. de Oliveira
International Space University, marta.oliveira@community.isunet.edu

Paulo J. S. Gil
CCTAE, IDMEC, Intituto Superior Técnico,
Universidade de Lisboa, paulo.gil@tecnico.ulisboa.pt

Richard Ghail
Imperial College London, r.ghail@imperial.ac.uk

September 2016

Abstract

In space exploration, planetary orbiter missions are essential to gain insight into planets as a whole, and to help uncover unanswered scientific questions. In particular, the planets closest to the Earth have been a privileged target of the world's leading space agencies. EnVision is a mission proposal with the objective of studying Earth's closest neighbor. Designed for Venus and competing for ESA's next launch opportunity, the proposal already went through the selective technical review for the M4 launch opportunity, and was submitted to the M5 call, incorporating feedback from ESA. The main goal is to study geological and atmospheric processes, namely surface processes, interior dynamics and atmosphere, to determine the reasons behind Venus and Earth's radically different evolution despite the planets' similarities. To achieve these goals, the operational orbit selection is a fundamental element of the mission design process. The design of an orbit around Venus faces specific challenges, such as the impossibility of choosing Sun-synchronous orbits. In this paper, an innovative genetic algorithm optimization was applied to select the optimal orbit based on the parameters with more influence in the mission planning, in particular the mission duration and the coverage of sites of interest on the Venusian surface. After summarizing the EnVision proposal's mission concept for Venus, the optimization and innovation of the operational orbit design will be analyzed in terms of its benefits to the mission.
Keywords: operational orbit, orbit design, scientific requirements, targets coverage, orbit optimization, genetic algorithms, Venus.

1. Introduction

1.1. Objective

The main objective of this paper is to improve the design of the operational science orbit around Venus for EnVision, the proposed medium class mission for the European Space Agency's Cosmic Vision 2015-2025 M5 call. The different requirements and constraints that affect the orbit design are analyzed to select and refine mission features, in particular the observation of selected targets within the shortest possible mission duration.

1.2. Studying Venus from Orbit with EnVision

The operational orbit is the orbit from which the mission's scientific observations are made. After an analysis of the space environment (third bodies, solar radiation pressure, micrometeorites, space debris, the planet's atmospheric drag, gravity), the operational orbit can be selected to satisfy instruments and scientific requirements (data resolution, coverage, revisit time, link budgets, eclipse duration, etc.). Often these requirements are contradictory and a prioritization balance must be made [1, 2].

Terrestrial planets closest to Earth are popular targets for orbiter missions [3]. Venus is often considered Earth's twin in terms of its size, distance from the Sun and bulk composition; though a great number of fundamental questions, such as the planet's geology and its correlation to the atmosphere are still unanswered [4].

EnVision builds on the discovery of geological activity made by Venus Express to identify and measure areas of geological activity on Venus and their relationship to atmospheric and interior processes [4] by providing gravity and geoid data, as well as new spin rate measurements. These science goals lead to specific observational objectives: surface change, geomorphology, specified targets, thermal emissivity, gravity field, spin rate and spin axis, among others.

A key objective is the observation of sites of interest on the surface of Venus, to link local surface observations to global features. For instance, surface images captured by Soviet Venera landers reveal pyroclastic or sedimentary deposits and not the basaltic lava flows assumed previously [4].

The major limitation with the present data is resolution: more accurate measurements are needed to distinguish the presence of different surface materials. There are many data issues and missing information [4]. The most significant specified targets are the Venera landers that were launched by the Soviet Union between 1961 and 1984 and consist essentially of approximately 2 m metal spheres with a landing ring and antenna coil [4]. Their size and metallic nature mean that the landers will appear 6 dB brighter than the rest of the surface in high resolution radar imagery [4].

The mission is planned to launch in October 2029 and following aerobraking, the orbiter was nominally interred for a low circular operational orbit at an altitude of 258 km. The payload includes [4]:

- A phased array synthetic aperture radar (VenSAR);
- A subsurface radar sounder (SRS);
- An infrared mapper and spectrometer (VEM); and
- A 3 m X/Ka band high gain antenna.

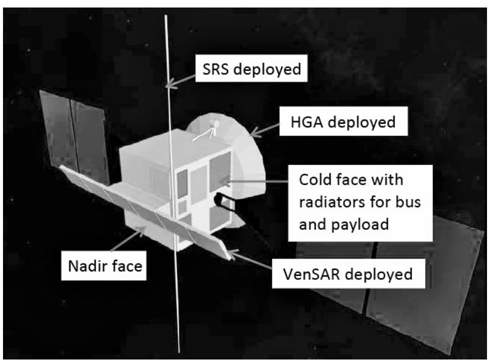

Figure 1: Preliminary operational configuration of EnVision's orbiter.[4]

EnVision will provide topographic and subsurface data with a better resolution than previous missions, and may uncover the reasons for the radically different evolution of Venus and Earth.

2. Operational Orbit Design Fundamentals

In this section, the fundamental concepts behind the orbit design will be introduced to support the orbit analysis and determination.

2.1. Design of an Operational Orbit around Venus

Mass	$4.9.10^{24}$ kg
Radius	6051.8 km
Surface Temperature	462° C
Revolution Period	224 days
Rotation Period	243 days
Number of Moons	none
Atmosphere	carbon dioxide, nitrogen

Table 1: Venus facts summary.

Venus has no natural satellites, simplifying the gravitational environment of the problem, and its rotation is retrograde. Also, the planet's path around the Sun takes around 224 days but takes 243 days to complete a full rotation around its axis, which results in a Venus year being shorter than a Venus day. Indeed the planet's rotation is extremely slow and has the slowest angular velocity in the Solar System (2.99×10^{-7} [rad/sec]) [8].

In Venus the gravitational perturbations are very small when compared to Earth. Indeed, the most significant gravitational perturbations term J_2 (4.458×10^{-6}) has still a value of only about 0.4 % of Earth's value [3]. This reduced perturbations effect is related to the fact that Venus' flattening coefficient is very close to 0 [9], so orbit apse rotation and nodal regression are very small. Essentially, Venus is almost perfectly spherical, it's the most spherical planet in the Solar System. This is in turn connected to Venus' extremely low rotation rate.

2.2. Orbit Representation

In this work, we used the Classical Orbital Elements to describe the orbits (longitude of the ascending node Ω, argument of perigee ω, inclination i, true anomaly ν_0, semi-major axis a, eccentricity e). We will focus on near circular and circular orbits.

In the case of the circular orbit, there is no periapsis, and consequently no argument of periapsis, or true anomaly. In order to correct the absence of the periapsis as a reference, we use the argument of latitude u, which can be related to the argument of peripasis and true latitude through the following expression: $u = \omega + \nu$. Essentially, the argument of latitude u is measured from the ascending node to the spacecraft's position in the direction of the spacecraft's motion [6].

2.3. Orbit Propagation

Venus is a complex case to apply the typically used orbits for remote sensing missions. For instance, the extremely low perturbations don't provide the torque that the gravity field of more oblate planets present to generate Sun-synchronous orbits [3]. Venus is the planet for which the spherical approximation is most accurate in the solar system [9].

Only low orbits (below 350 km) were considered viable for the EnVision mission which consequently helps reduce the fuel required for solar perturbations corrections [4]. Moreover, we only examined altitudes above 230 km as was recommended in the proposal to avoid the sensible atmosphere detected by Magellan and Venus Express below 200 km [4].

For the purpose of this work the perturbations are small enough or corrected in a way that makes it possible to consider only Keplerian orbits, where only the true anomaly element changes, determined by Kepler's equation.

3. Orbit Design and Optimization Approach for EnVision

In this section, the procedure adopted to implement the orbit optimization will be described, from the provisional orbital parameters computation to the algorithm selection and application.

3.1. Mission Constraints

As mentioned in the previous section, one of the main objectives of the mission is to observe the specified sites of interest on the surface of Venus, in particular, the Venera and Vega landers. The observation of these targets will give us the ground truth. In Table 2, the targets are listed with the corresponding priority level (1 being the highest level). We will also focus on the North Pole interferometry measurements that will be necessary for many science goals such as spin axis and rate.

Target	*Latitude*	*Longitude*	*Priority*
Vega 1	7.2° N	177.8° E	2
Vega 2	7.14° S	177.67° E	2
Venera 5	3° S	18° E	3
Venera 6	5° S	23° E	3
Venera 7	5° S	351° E	3
Venera 8	10.70° S	335.25° E	2
Venera 9	31.01° N	291.64° E	1
Venera 10	15.42° N	291.51° E	1
Venera 11	14° S	299° E	3
Venera 12	7° S	294° E	3
Venera 13	7.5° S	303° E	1
Venera 14	13.25° S	310° E	1

Table 2: Target sites.

The scientific requirements demand a well-controlled near circular orbit (with a maximum eccentricity of 0.001) [4]. Also, the altitude should be as low as possible since the resolution of the gravity field declines rapidly with altitude. In terms of the atmospheric drag effect, previous missions detected sensible atmosphere below 200 km altitude: an altitude not below 230 km was considered adequate [4].

The primary instrument carried by EnVision is VenSAR, which has five operating modes. The modes used in this study are interferometry and high resolution strip-mode. The geometries for these modes depend primarily on the swath width and incidence angles. The area covered by the antenna is the footprint, and the swath width refers to the strip of Venus' surface from which the mission data is being covered (figure 4). VenSAR has a fixed axis of maximum radiated power of 32° .

Parameter	Interferometry	Strip-mode
Swath Width	43 km	40 km
Incidence Angle (near)	38.2°	36.3°
Incidence Angle (far)	44.1°	42.2°

Table 3: VenSAR operating modes parameters and coverage.

3.2. Orbit Dynamics with Provisional Parameters

To test and simulate the orbit dynamics we first considered the provisional EnVison orbit parameters.

Ω	e	i	u	a (altitude)
0°	0	88°	195°	6309.8 km (258 km)

Table 4: Provisional orbit parameters.

In the visualization of the spacecraft's ground track we included the target sites to have a more intuitive tool regarding the observation of these targets. The sites of interest plotted were the landers Vega 1,2 and Venera 5, 6, 7, 8, 9, 10, 11, 12, 13, 14.

The Venus rotation speed is very small as was stated before. Modeling the mission time can be rather slow, since the time step shouldn't be greater than 100 seconds. The discontinuous appearance in the trajectory lines for the five days ($\sim$ 80 orbits) is related to the fact that we chose a time step of 100 s.

3.3. Observations Computation

In order to compute the observations of the target sites with VenSAR, it is necessary to examine valid geometry approximations.

The SAR antenna operates as a continuous swath (strip-mode) to detect the targets, and the targets observations computation was scripted and approached as follows:

- We considered an approximation of a flat surface model that comes with a total error of

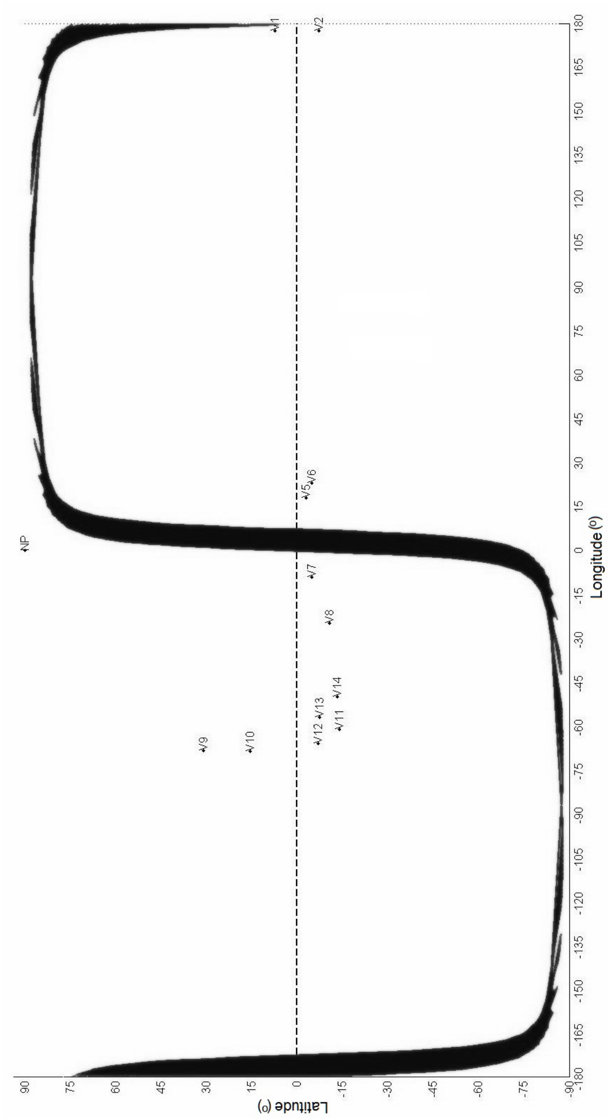

Figure 2: Ground track plot for five days (∼ 80 orbits) at 100 s step for provisional parameters showing the result of Venus' small rotation speed.

around 4 km when compared with the spherical model swath results from the proposal (figure 4);

- The footprint was assumed to be equal to the swath width, i.e. if the target is inside the swath width, we can assume it can be observed;

- In order to take into account the deviations and to make sure that the target site is not just intersected at the swath edge we considered a width of 30 km, equivalent to 0.3 ° (33 km for the North Pole) for the initial scenario with the provisional parameters;

- Since for testing the observations, the VenSAR with nadir direction is interesting to consider for its simplicity, both nadir and off-nadir geometries were calculated (only the off-nadir geometry represents the operational SAR);

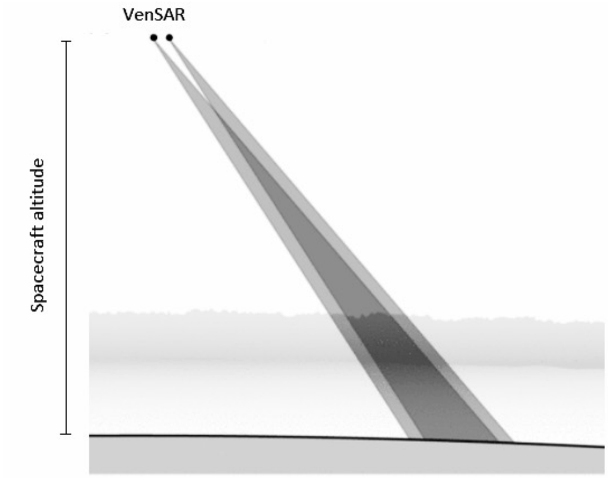

Figure 3: VenSAR's interferometry mode.

- The off-nadir geometry corresponding to the high resolution mode that will be observing the targets was scripted with incidence angles of 36.3° and 42.2° (44.1° and 42.2° for the North Pole interferometric measurements);

- Finally, the swath width is given by $y - x$, and from the altitude and the tangent relations that give us x and y, we can estimate the swath and the distance between the "VenSAR sub-point" (VSSP) longitude and the spacecraft sub-point (SSP) longitude $d_{\text{VSSP}} = x + \text{swath}/2$.

The "VenSAR sub-point" (VSSP) represented in figure 4 corresponds to the spacecraft sub-point (SSP) corrected for the VenSAR observations track. In brief, since the strip SAR image dimension is limited across track, if the VSSP is between [Target's longitude - swath/2 ; Target's longitude + swath/2], the target is considered observed.

3.4. Optimization Problem Formulation

We want to observe the targets with high priority as soon as possible in a minimum time, while satisfying the orbit constraints (near polar, near circular, low altitude). This way we ensure that the main targets are observed at the beginning of each mission cycle (1 cycle corresponds to a Venus period) and that the operations planning for VenSAR will be easier.

3.5. Optimization Method Selection

To solve our optimization problem, we need global optimization, i.e. a method that seeks to find the global best solution of an objective function that translates our goals while satisfying the orbit constraints. We refer to the optimization as global

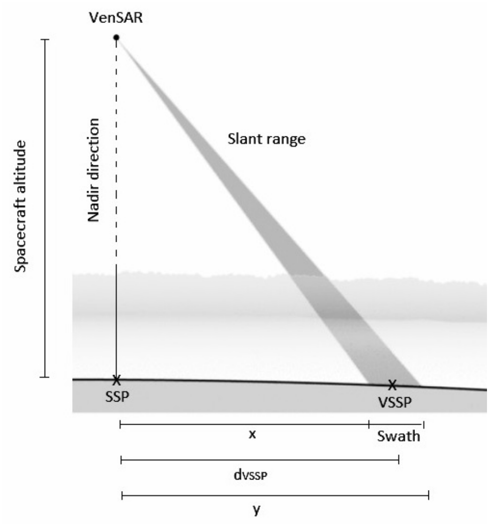

Figure 4: Geometry approximation for VenSAR in strip-mode.

since our objectives will likely lead to an objective function with multiple local optima.

In the presence of multiple local minima, if we use traditional local scope search methods we will often find locally optimal solutions [10]. To obtain a globally optimal solution, there are exact methods, in particular deterministic methods, which always produce the same output for a given input and don't involve randomness, and stochastic methods, that use randomness. But there are also heuristic methods, which look for solutions among all possible ones, but do not guarantee that the best solution is found [10].

Recently, genetic algorithms have proven to be a very successful way of getting solutions in orbit design optimization problems similar to the one addressed in this study. We have summarized some of the advantages of selecting the genetic algorithm to optimize the orbit design:

- The proven success of the method for problems that are not convex, having many local minima [11, 12];
- The possibility of combining code for integer, real values and options [11];
- The fact that the algorithm's randomness can accelerate the progress of the optimization, and can make the method less sensitive to modeling errors [13];
- Finally, the possibility that the randomness can lead to a global optimum by escaping a local minimum.

3.6. Genetic Algorithm Implementation

The unknown variables considered for the optimization are:

- Longitude of the ascending node Ω;
- Argument of perigee ω;
- Inclination i;
- True anomaly ν_0;
- Semi-major axis a;
- Eccentricity e;
- And finally, the time it takes to observe the mission's targets tf.

To fulfill the main objective identified, we need to select the fitness function that will be minimized by the genetic algorithm for the input boundaries we define. The fitness function will translate the mission duration and the targets observation objective with computational efficiency.

We want to observe the targets with high priority (Venera 8, 9, 10, 13, 14, Vega 1, 2) as soon as possible in a minimum time, while satisfying the orbit constraints. Additionally, we want to observe the landers Venera 5, 6, 7, 11, 12. After the objectives and computational efficiency analysis, we selected the following fitness function F_i to evaluate our main objective

$$F_i = -\alpha \frac{N_i(\Omega, \omega, i, \nu_0, tf, a, e)}{N} + \beta \frac{tf_i}{T_{Venus}}, \quad (1)$$

where N_i and tf_i are the fitness terms for the i^{th} design point, N_i is the total number of observed sites in tf_i seconds, α and β are the fitness weight parameters (values between 0 and 1), which translate the relative importance of the fitness terms (maximizing number of covered sites versus minimizing the time needed), N is the total number of target sites considered, and finally T_{Venus} is Venus' period.

As was stated before, modeling mission times for Venus is very slow, because the time step has to provide enough time to pass above the area of interest. Due to extremely different scales of the number of intersections and the mission durations the genetic algorithm will tend to kill populations with high mission durations if the fitness function weights don't compensate, that is why α and β are necessary. This effect could result in an optimal solution with minimum time window but losing focus of the number of intersections, which is why it is necessary to use different combinations of the fitness function.

The total number of observed sites N is obtained from the observations computation, i.e. if the target is inside the swath width, we can assume it was observed. Considering only the sites with priority, we have $N = \sum_{n=1}^{8} T_n$ with $T_n = 1$ if the target n is observed, and $T_n = 0$ if the target n is not observed. N_i is a dependent variable that can be computed given the candidate orbit and the set of sites to select from. The reason why we divide N_i by N and tf_i by T_{Venus} is so that we get better scaled fitness function values.

To describe the implementation of the genetic algorithm function it is fundamental to go over a few options that were made. We defined the population size to 100 individuals in each generation, since it was a good compromise between convergence efficiency and computational cost. The algorithm runs until the average relative change in the fitness function value above the minimum stall generations (default value of 50) is less than the function tolerance TolFun (with set value of 1×10^{-4}). If $|f(xi)–f(xi+1)| <$ TolFun, the iterations stop [14].

4. Optimization Results

4.1. Algorithm Tests and Validation

We tested the script in order to evaluate the fitness function's convergence with the conditions in table 5.

Ω bounds	[0° - 360°]
ω bounds	[0° - 360°]
i bounds	[-90° - 90°]
ν_0 bounds	[0° - 360°]
tf bounds	[1000000 s - 10000000 s]
a bounds	[6300 km - 6400 km]
e bounds	[0 - 0.01]
α	1
β	1
Targets	Venera, Vega landers, North Pole
Geometry	Nadir

Table 5: Fitness function test conditions.

Ω	272.779°
ω	342.080°
i	-49.714°
ν_0	126.598°
tf	5670319.015 s
a	6390.834 km
e	0.001
Targets	12/13

Table 6: Best solutions obtained $F_i = -0.653$ for the fitness function test conditions.

We plotted the minimum, maximum, and mean fitness function values in each generation for the selected fitness function F_i, and observed the convergence ($|f(xi)–f(xi+1)| <$ TolFun) after a few more than 50 generations. As expected the Best, Worst values bars decrease progressively until the fittest solution is reached.

We also wanted to see how the solutions F_i of the fitness function varied with the change in design variables, and for that purpose separate metric studies were performed to investigate the variation of the fitness function with the orbital elements i, Ω, ω and the time variable tf (figures 6 and 7). It is interesting to highlight that in figure 6, we can observe an expected symmetry in the fitness function dependency of inclination, and no targets are covered for an equatorial orbit.

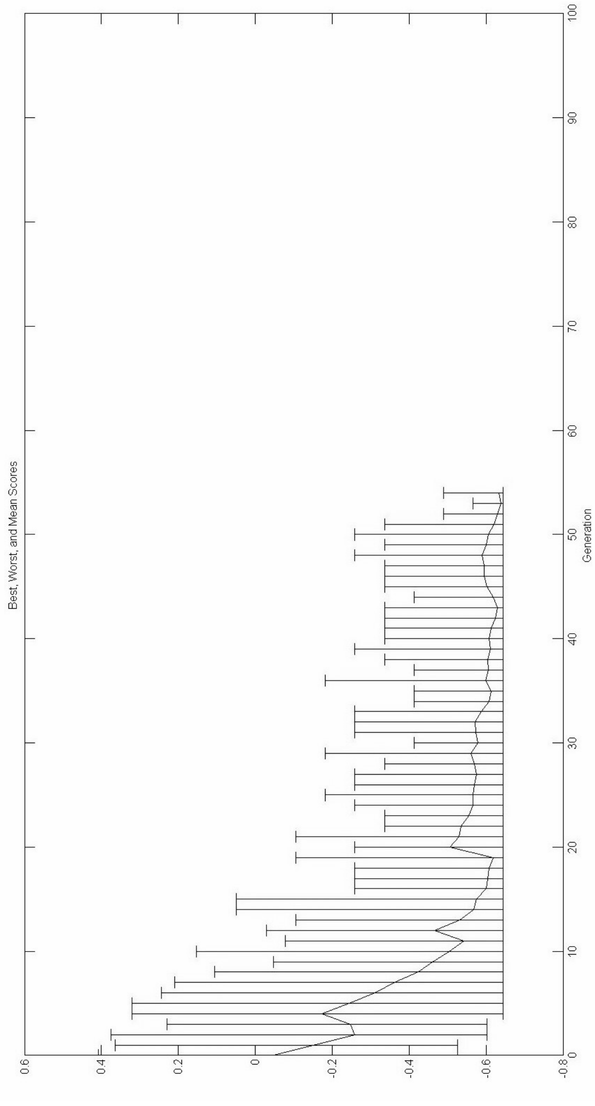

Figure 5: Minimum, maximum, and mean fitness function values versus generations for fitness function test conditions.

Furthermore, in figure 6 we observe that for the near polar inclinations the fitness function value increases. This is related to the fact that not as many targets are covered for the these inclinations for short durations, which is expected since in this case the optimization is taking into account equal weights both fitness terms. Most targets are located near the equator, so for shorter mission times the algorithm should lead to a fittest solution with a lower inclination. The ground track of an orbit with lower inclination covers a larger area around the equator than near polar orbits.

Naturally, with these conditions, we only get 12 out of the 13 targets covered, since the North Pole is not observed. The fittest solution obtained has an inclination of $i = -49.714°$ (Table 6). In figure 6 we can observe a peak around that inclination value, corresponding as expected to a global minimum peak. The Ω value associated to that peak corresponds to the fittest solution value. In figure 7, we can also identify the global minimum peak associated to the fittest solution's tf and ω values.

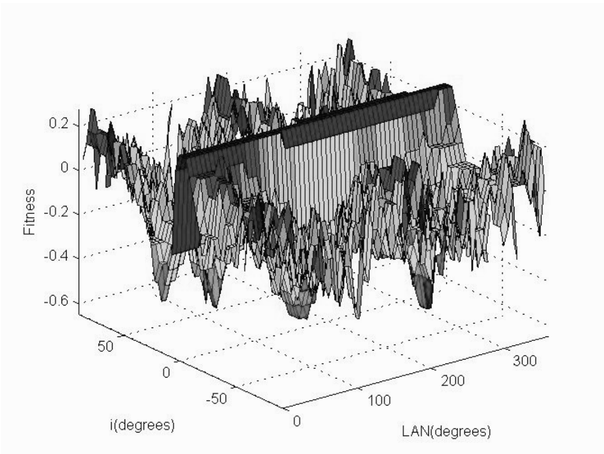

Figure 6: F_i versus inclination i and longitude of ascending node Ω for the fitness function test conditions.

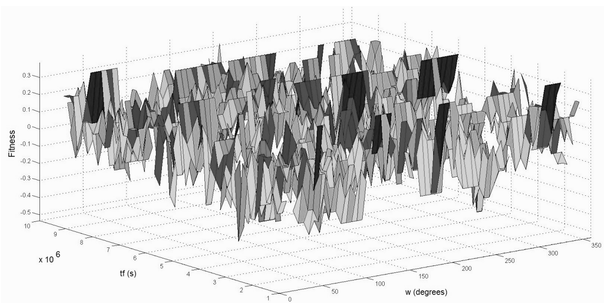

Figure 7: F_i versus time window tf and argument of perigee ω for fitness function test conditions.

After observing the fitness function, it is also necessary to further test the algorithm implementation. For that purpose, we used a simple test with a larger and fixed footprint of 5° to target just the Venera landers with the nadir geometry for its intuitive nature (Table 7). These set conditions provide us the opportunity to quickly test the algorithm for short durations, since it should very quickly find a solution that covers these targets with a low inclination orbit (the same weights were attributed to the fitness terms). These conditions are set just to test the validity of the algorithm implemented, since it does not satisfy many of the mission constraints (polar coverage, e inferior to 0.001). We plotted the best and mean function values in function of the generation to observe the convergence (figure 5). In this case, as expected, due to the large footprint considered, the lower the inclination the faster the Venera landers near the equator are covered, which explains the parametric plot in figure 9 and the fittest solution obtained (table 8).

Ω bounds	[0° - 360°]
ω bounds	[0° - 360°]
i bounds	[-90° - 90°]
ν_0 bounds	[0° - 360°]
tf bounds	[10000s - 100000s]
a bounds	[6300km - 6400km]
e bounds	[0 - 0.01]
α	1
β	1
Targets	Venera landers, North Pole
Geometry	Nadir altered with fixed 5° footprint

Table 7: Test conditions for short durations.

Ω	246.470°
ω	233.501°
i	9.281°
ν_0	151.388°
tf	10595.253s
a	6390.834km
e	0.001
Targets	8/11

Table 8: Fittest solution $F_i = -0.727$ for short durations test conditions.

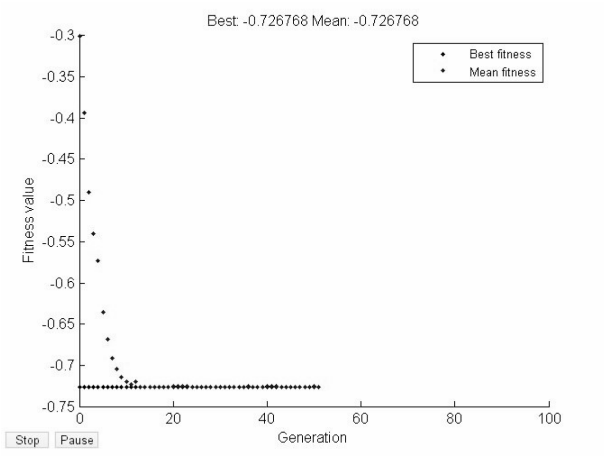

Figure 8: Best and mean fitness function values versus generation for short durations test conditions.

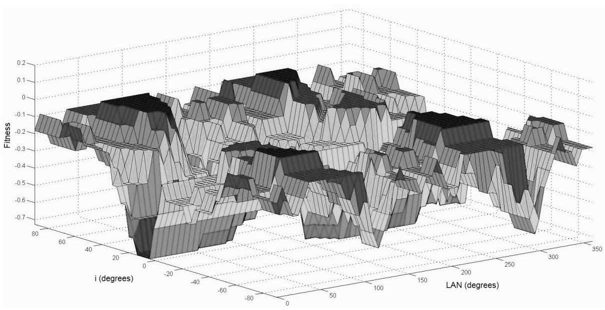

Figure 9: F_i versus orbital parameters i and Ω for short durations test conditions.

4.2. Optimal Solution

When searching for an optimal orbit solution, we took into account the priority established for the target sites, and only considered Vega 1, 2, Venera 8, 9, 10, 13, 14 and the North Pole observations. In order to ensure that all targets with high priority were covered, the fitness function weight coefficients considered were $\alpha = 0.7$ and $\beta = 0.3$. The other conditions are summarized in Table 9.

Ω bounds	[0° - 360°]
ω bounds	[0° - 360°]
i bounds	[87° - 90°]
ν_0 bounds	[0° - 360°]
tf bounds	[1000000s - 10000000s]
a bounds	[6300km - 6400km]
e bounds	[0 - 0.001]
Geometry	Off-Nadir

Table 9: Test Conditions for EnVision.

In a next step, we checked separately with the targets observation script that with this orbit it is possible to cover all 13 targets just after 1000 orbits, so almost two times faster than with the provisional parameters considered in the EnVision proposal. Furthermore, the first observation is immediately achieved during the mission's first orbit. We calculated the main features of the optimal orbit obtained including the spacecraft altitude of 259.028 km, the spacecraft velocity of 7.1747 km/s, and the orbital period of 5526.65 s. Even though the spacecraft's orbital period remained closely the same as in the previous proposal, the interest sites are optimally covered at the start of the first cycle, and it is possible to reduce the total number of cycles needed for the mission and still repeat the coverage of the sites.

Ω	285.789°
u	351.669°
i	88.163°
tf	5571678.038 s
a	6310.828 km
e	0.000
Targets	8/8

Table 10: Fittest solution $F_i = -0.700$ for an optimal orbit solution.

To visualize the optimal orbit we plotted the ground track (figure 10). After 155 Orbits we can check on the ground track that four sites were intersected (Venera 9, 10, 12 and North Pole).

Overall, the optimality of the method was verified in the sense that the heuristic returned an optimized solution. We evaluated the quality of the solutions through numerous algorithm tests and the convergence of the method was determined by TolFun. With the fittest solution obtained we observe all targets in a good time and as soon possible.

5. Conclusions

In this study, we investigated EnVision's operational orbit and optimized it for the observation of selected targets. The problem formulation was developed to design an orbit that covers as many of the target sites as possible, while minimizing the time window in which these observations are performed. A genetic algorithm was implemented to evaluate the combinatorial coverage problem.

Overall, the optimization method selected was a success in finding a fit solution to EnVision's case study. We investigated the algorithm's fitness function's dependence on the different orbital elements and time variable and obtained an operational orbit that ensures the coverage of the sites of interest on the surface of Venus as early as possible.

Even though the metric, constraints and priorities considered are specific to the EnVision mission, the main scripts developed in this study can be adapted to other orbiter missions to Venus and even to other planets with the right adaptations,

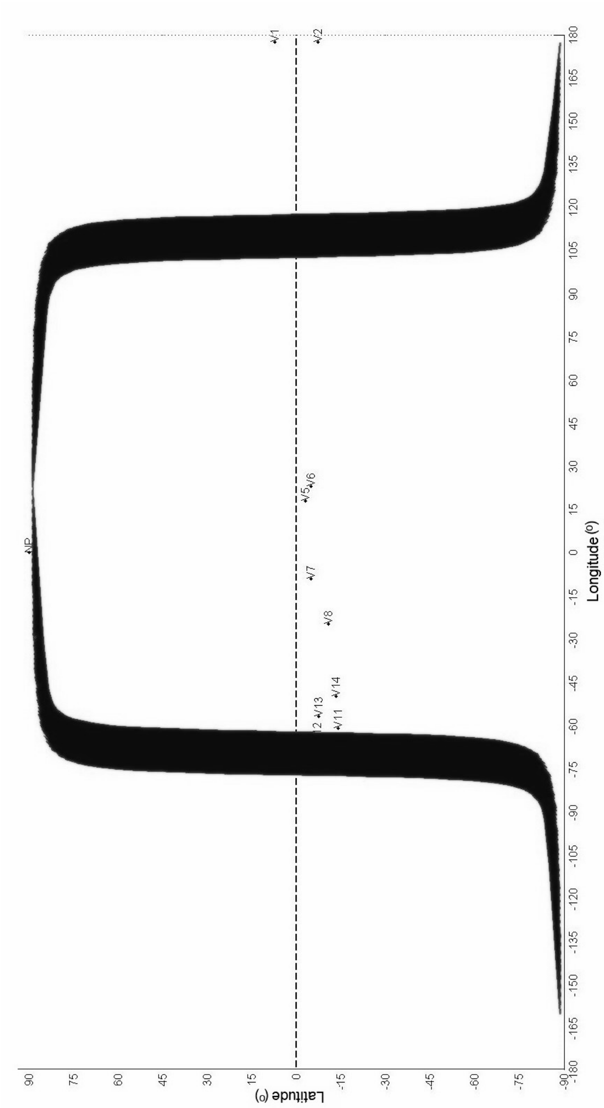

Figure 10: Ground track plot for 10 days ($\sim$ 155 orbits) at 100 s step for optimal orbit.

as the intersection computation and optimization procedure might be similar.

The results of this study were first introduced in the EnVison session during the European Planetary Science Congress in September 2015, and were included in the mission proposal to ESA. Further research on this subject will be developed as the mission's science and payload team refine their data. It will be possible to evaluate other objectives such as telecommunications, spotlight mode coverage, and propulsion metrics applied to the natural orbit.

Acknowledgements

M.O. would like to thank the EnVision team for the collaboration opportunity and the NAIF team from JPL for the support provided.

The work of Paulo J. S. Gil was supported by FCT, through IDMEC, under LAETA, project UID/EMS/50022/2013.

References

[1] J. Wertz et al., *Space Mission Analysis and Design*, 3rd edition, Space Technology Library, 1999.

[2] S. Kemble, *Interplanetary Mission Analysis and Design*, Springer, 2006.

[3] P. Anderson et al., *Novel orbits of Mercury, Venus and Mars enabled using low-thrust propulsion*, Acta Astronautica vol. 94, pp. 634–645, 2014.

[4] R. Ghail et al., *EnVision - Understanding why our most Earth-like neighbour is so different*, ESA Cosmic-Vision 2015-2025 M5 Call Mission Proposal, 2015.

[5] D. Titov, *Venus Express science planning*, Planetary and Space Science, vol. 54, pp. 1279-1297, 2006.

[6] *Spacecraft Attitude and Orbit Control*, 3rd Edition, Princeton Satellite Systems, 2014.

[7] W. Wiesel, *Spacefilght Dynamics*, 3rd Edition, Aphelion Press, 2010.

[8] D. Williams, *Venus Fact Sheet*, NASA, April 2015. `http://nssdc.gsfc.nasa.gov/planetary/factsheet/venusfact.html`

[9] B. Archinal, *Report of the IAU Working Group on Cartographic Coordinates and Rotational Elements:2009*, Springer Science Business Media B.V., Oct 2010.

[10] D. Whitley, *A Genetic Algorithm Tutorial*, Statistics and Computing, pp. 65-85, 1994.

[11] O. Abdelkhalik and A. Gad, *Optimization of space orbits design for Earth orbiting missions*, Acta Astronautica vol. 68, pp.1307–1317, 2011.

[12] S. Lee et al., *Orbit Design and Optimization Based on Global Telecommunication Performance Metrics*, Jet Propulsion Laboratory, 2011.

[13] H. Hoos et al., *Stochastic Local Search: Foundations and Applications*, Morgan Kaufmann/Elsevier, 2004.

[14] *Genetic Algorithm Options*, Mathworks. `http://www.mathworks.com/help/gads/genetic-algorithm-options.html`